Journal of
Ceramic Science
and Technology

J. Ceram. Sci. Technol. 1-10 (2019)
DOI: 10.4416/JCST2019-00048
available online at: http://www.ceramic-science.com

Design and Experiment of a 3D Printing System for Ceramics by Continuous Extrusion

Y. CHAO*[1], X. LIU[2]

[1]College of Mechanical and Electrical Engineering, Xuchang University, Xuchang 461000, China
[2]Xuchang Tobacco Machinery Co. Ltd, Xuchang 461000, China

received June 24, 2019; received in revised form August 12, 2019; accepted August 14, 2019

Abstract

In order to solve the problems of the brittleness, high hardness, complex shapes, long production times and high cost of ceramic parts, a novel 3D printing system for ceramics is proposed for the fabrication of ceramic parts by means of continuous extrusion. Based on an analysis of the principle of continuous extrusion of ceramics as a forming process, the system structure, nozzle extrusion device and motion control system were developed. The influence of the process parameters on the quality and defects of printed parts was analyzed in a series of printing experiments. The causes of defects (tiny cracks, porosity, holes and irregular morphology) were explored and summarized. Precise contours, size and high bonding quality can be obtained when the printing speed is matched well to the speed of ceramic extrusion. Vases and model heads were fabricated using the 3D printing system. The results of the experiments show that the 3D printing system can meet the precision requirements for ceramic parts. The feasibility and correctness of the 3D ceramic printing technique are verified.

Keywords: 3D ceramic printing, continuous extrusion, nozzle extrusion device, bonding quality.

I. Introduction

Ceramic materials have been widely used in military and civil fields [1] because of their inherent physical and chemical properties. However, owing to their brittleness, poor toughness and machinability, traditional ceramic parts are mostly fabricated by means of hand throwing of clay, pressure casting and other methods [2]. The complexity of the ceramic part shape is limited, the production cycle is long, and the cost is high, on account of the restrictions of casting molds and cutting tools.

For this reason, a novel process for forming ceramic parts has been designed and developed to reduce production costs and realize complex-shaped ceramic parts, which has become a key problem. In recent years, the emergence of 3D printing technology has provided an effective solution for forming ceramic parts with a complex shape. 3D printing is an additive manufacturing (AM) [3] process, any part with a complex shape can be fabricated by materials being piled up layer by layer based on a three-dimensional model of the part.

3D printing of ceramic material has the following significant advantages [4–7]: (1) No need for a casting mold and cutting tools, short production cycle and low manufacturing cost; (2) Any complex shape or structure can be fabricated, the constraint of traditional manufacturing geometry no longer applies; (3) Suitable for personalized customization and small batch production; (4) A wide range of materials, such as zirconia, alumina, ceramic matrix composites, clay and resin-based ceramic slurry, can be printed. At present, 3D printing technologies used to fabricate ceramic parts mainly include the following five process methods. Selective Laser Sintering (SLS) ceramic powder process [8], Continuous digital light processing (DLP) ceramic 3D printing [9], Ceramic slurry spraying deposition [10], Adhesive spraying and bonding ceramic powder process [11], Ceramic stereolithography apparatus (SL) [12]. After years of development, great progress and breakthroughs have been made in 3D printing of ceramics. Currently, 3D printing machines for ceramic are popularly commercialized by companies such as ExOne and 3D Systems [13]. However, various challenges [14–17] in 3D printing technologies for ceramics still need to be faced, such as low printing efficiency; defects such as cracks and deformation; poor mechanical properties, yield and precision of the parts formed. In a word, each forming method mentioned above has different material requirements, fields of application and equipment functions. The forming processes should be further optimized for practical application.

In this paper, a convenient and effective method is proposed to fabricate ceramic parts by means of continuous extrusion of ceramic and its deposition layer by layer. The structure, nozzle extrusion device and motion control module for a 3D printing system for ceramics were developed. A series of printing experiments was conducted to analyze the influence of the process parameters on the quality and defects of printed parts. The correctness and

* Corresponding author: chaoyanpu@163.com

feasibility of the ceramic 3D printing technique have been verified.

II. Forming Principle and Experiment System

The 3D printing of ceramics by means of continuous extrusion is a novel method for preparing ceramic bodies. The forming principle is as follows: the ceramic clay is firstly loaded into a storage silo, under the action of air pressure; the ceramic body is transported through a pipe to the nozzle device. The extrusion screw is driven to rotate by a stepper motor; the ceramic body is continuously extruded from the nozzle to form clay filaments. The clay filaments are deposited layer by layer according to the data information of the CAD model of the part. Finally, the ceramic parts are obtained after the post-treatment processes of drying and sintering.

According to the forming principle and process characteristics, the ceramic 3D printing system must have the following functions: (1) The ceramic body is continuously transported through the pipe to the nozzle device, in order to provide raw materials for subsequent extrusion; (2) The ceramic body can be continuously extruded to form clay filament, and the size of the clay filament can be precisely controlled to satisfy the requirements of the subsequent printing deposition; (3) The trajectory of scanning deposition is effectively controlled according to the data information for the part being formed; (4) The extrusion and deposition process is monitored online, which provides a basis for the adjustment and selection of the printing parameters; (5) The temperature of the deposition substrate must be precisely controlled to provide a temperature environment that satisfies the process requirements for clay deposition and solidification. According to the overall function of the above experiment system, the ceramic extrusion 3D printing deposition system was designed and developed, as shown in Fig. 1. The ceramic extrusion system is composed of a stepper motor, an extruding screw and an extrusion nozzle. The extruding screw is driven to rotate by the stepper motor. Under the extrusion pressure of the extruding screw, the ceramic body is extruded through the nozzle at the bottom to form clay filament. The control system for the forming trajectory is composed of a three-dimensional motion platform, servo driver, multi-axis controller, measuring device and control software. With the full closed-loop control mode, the deposition path of the clay filament is precisely controlled. The temperature control system is composed of a heating device, a k-type thermocouple and a temperature control instrument. The temperature of deposition substrate can be accurately measured and controlled by the temperature control system during the forming process. The raw material conveying system is composed of an air pump, pressure-regulating valve, storage silo and pipeline. Under the action of the set air pressure, the ceramic body is continuously transported to the extrusion chamber through the pipeline. In the printing process, the clay filament is deposited layer by layer on the substrate as the three-dimensional platform moves. Finally, the original ceramic part is fabricated completely.

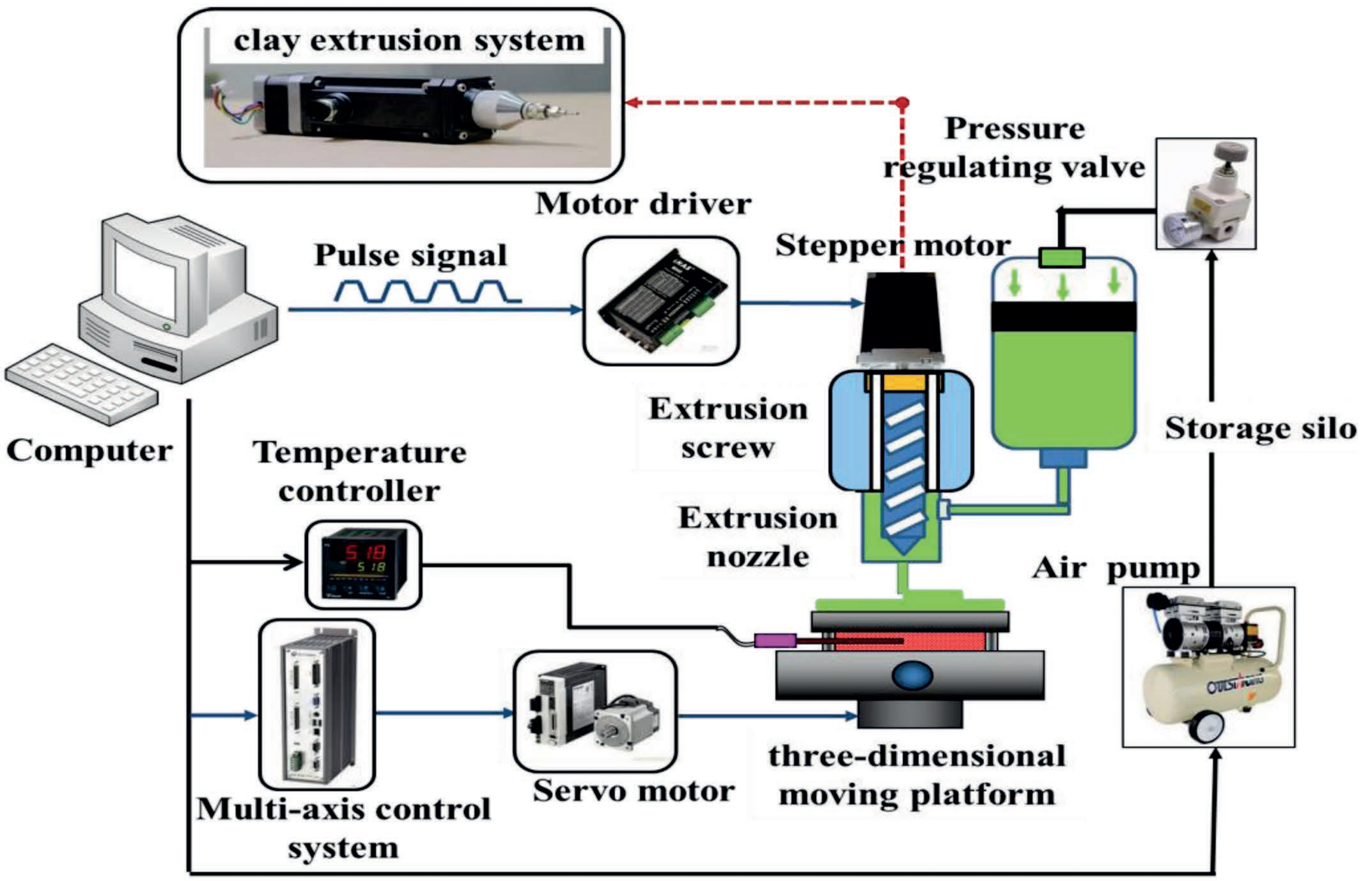

Fig. 1: Forming principle and experiment system.

III. Design of the Motion Control System

The motion control system is the key module of the ceramic 3D printing system. It is used mainly for outputting various instructions and signals in real time and receiving the real-time test data from various sensors. The actions of all moving parts and the depositing trajectories of the clay filament are controlled online in real time in the part-forming process.

The open structure based on a PC and motion controller was adopted in the experimental system for 3D printing of ceramics. An Advantech PC was chosen as the upper computer and a GOOGOL multi-axis motion controller was chosen as the lower computer. The four-channel motor control signals can be output. The maximum stroke of the three-axis motion platform is 300 mm in the X direction, 300 mm in the Y direction, and 200 mm in the Z direction. The repeat positioning accuracy of the three-axis motion platform is plus or minus 0.001 mm. A Yaskawa servo motor and the ball screw are used as the driving device for the motion platform. Renishaw RGH41 linear grating is used as position detecting element, and an Omron EE -SX674 photoelectric sensor is used as a limit switch. The man-machine control interface is developed by using a GOOGOL Otostudio software platform. The coordinate spacing, screw pitch, motor speed and acceleration can be set and displayed. The structure of the whole system is shown in Fig. 2, the upper PC communicates with the lower multi-axis motion controller through the dynamic link library and the device driver. The feedback from the raster ruler is received in real time, and the full closed-loop control of each axis is realized.

IV. Experiments and Analysis

In the process of fabricating ceramic parts, the forming wall thickness, side length and height of ceramic part are affected by many process parameters. In order to explore the influence of the process parameters on the forming quality and defects of fabricated parts, a series of experiments was conducted with different process parameters. The specific composition of the ceramic material used is Al_2O_3 18 %, SiO_2 72 %, K_2O 5.7 %, Na_2O 0.11 % and Fe_2O_3 0.7 %. The substrate temperature was set at 60 °C.

Fig. 3 shows the six samples printed with different process parameters. The standard design size of the sample is: 6.5 mm wall thickness, 60 mm side length and 70 mm height. The experimental process parameters of the six samples are shown in Table 1, all samples were fabricated under 0.25 MP extrusion pressure P_s. In addition, the slice thickness H_s of samples 1, 2 and 3 is 2.4 mm, the nozzle diameter D is 2.5 mm, and the printing speed V_p is 2 mm/s, 2.5 mm/s and 3 mm/s, respectively. The slice thickness H_s of samples 4, 5 and 6 is 2.2 mm, the nozzle diameter D is 2 mm, and the printing speed V_p is also 2 mm/s, 2.5 mm/s and 3 mm/s. Each measurement object (W_t, L_s and H) is measured six times in different position points of the sample, and the average values are calculated as shown in Table 2.

Table 1: The process parameters for the deposition of the parts.

Process parameters	Part numbers					
	1	2	3	4	5	6
Nozzle diameter: D (mm)	2.5	2.5	2.5	2	2	2
Slice thickness: H_s (mm)	2.4	2.4	2.4	2.2	2.2	2.2
Printing speed: V_p (mm/s)	2	2.5	3	2	2.5	3
Extrusion pressure: P_s (MP)	0.25	0.25	0.25	0.25	0.25	0.25
Extrusion speed: V_e (mm/s)	2.5	2.5	2.5	2.5	2.5	2.5

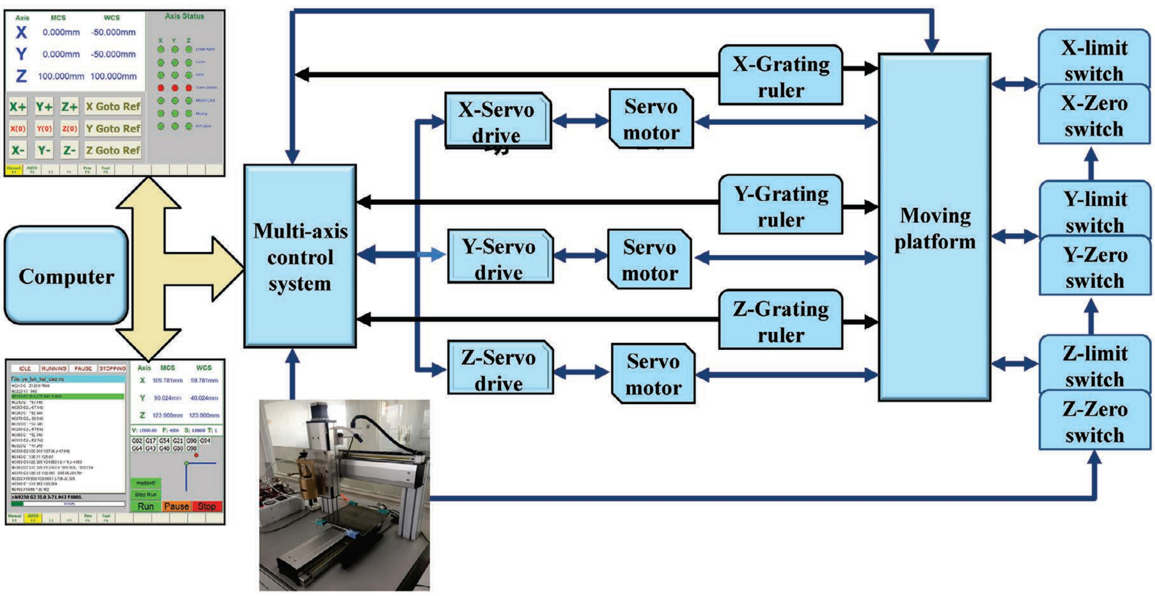

Fig. 2: The structure of motion control system.

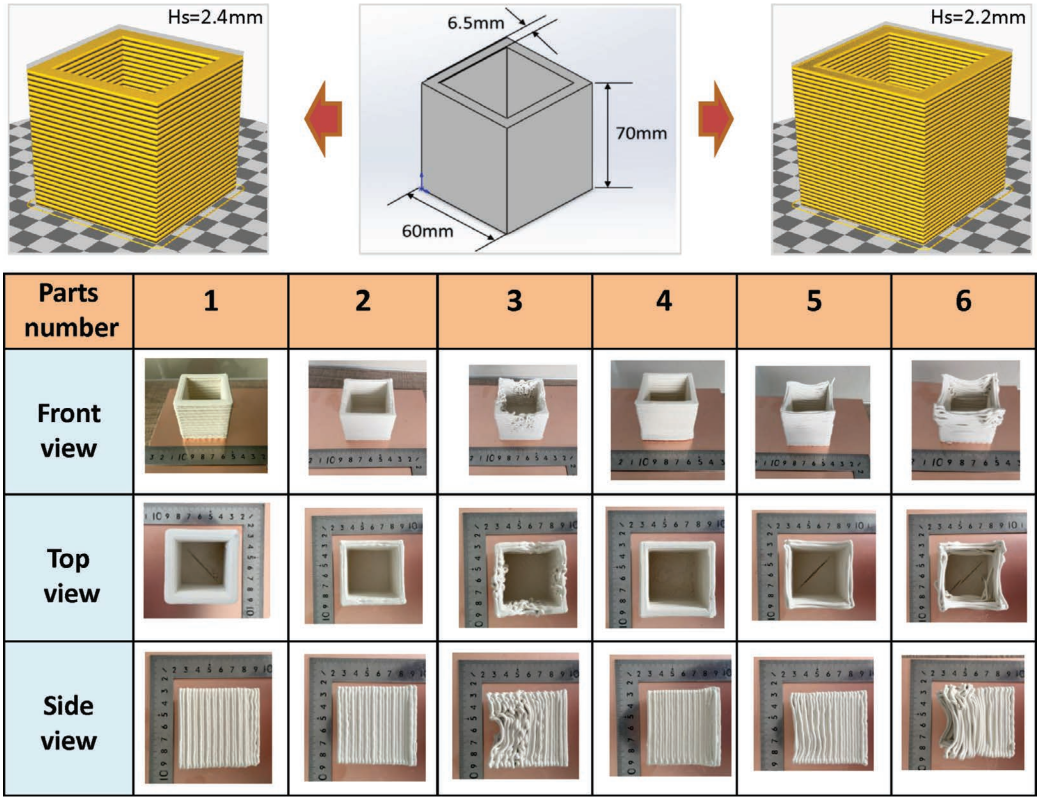

Fig. 3: The deposited parts with different process parameters.

Table 2: The measurement data of the deposited parts.

	Wall thickness: W_t(mm)				Length of side: L_s(mm)				Height: H (mm)			
1	Average: 10.9				Average: 65.3				Average: 71.3			
	1	11.5	4	11.2	1	65.1	4	65.4	1	71.5	4	71.6
	2	11.4	5	10.5	2	65.2	5	64.8	2	70.3	5	70.8
	3	10.6	6	10.4	3	65.8	6	65.5	3	72.2	6	71.4
2	Average: 6.8				Average: 61.6				Average: 71.3			
	1	6.4	4	6.5	1.	61.5	4	60.3	1	70.6	7	70.5
	2	7.2	5	7.8	2.	60.5	5	61.8	2	71.2	5	71.4
	3	6.8	6	6.2	3.	61.2	6	64.5	3	72.3	6	71.6
3	Average: 8.6				Average: 61.3				Average: 66.5			
	1	8.6	4	6.8	1	61.2	4	60.5	1	70.5	4	58.6
	2	7.2	5	10.2	2	61.4	5	60.8	2	63.5	5	71.2
	3	9.4	6	9.7	3	60.2	6	63.8	3	65.4	6	70.3
4	Average: 8.3				Average: 66.3				Average: 65.6			
	1	8.2	4	8.8	1	65.3	4	65.6	1	65.2	4	66.2
	2	8.6	5	7.8	2	66.4	5	66.2	2	65.8	5	64.8
	3	8.3	6	8.4	3	65.8	6	68.2	3	65.4	6	65.6
5	Average: 6.6				Average: 61.3				Average: 64.8			
	1	6.8	4	6.2	1	61.3	4	60.8	1	64.7	4	64.8
	2	7.2	5	6.4	2	60.6	5	60.5	2	65.2	5	64.6
	3	6.6	6	6.3	3	61.5	6	63.2	3	63.4	6	66.3
6	Average: 7.3				Average: 62.7				Average: 65.1			
	1	9.5	4	8.3	1	53.4	4	62.6	1	64.8	4	60.2
	2	6.2	5	5.9	2	68.7	5	64.5	2	72.5	5	63.4
	3	7.6	6	6.4	3	61.8	6	65.3	3	63.6	6	66.3

According to the measured average values, data point graphs are drawn, as shown in Fig. 4, Fig. 5, Fig. 6 and Fig. 7. Fig. 4 shows the six measurement results for the wall thickness in each part. Fig. 5 shows the six measurement results for the length of side in each part. Fig. 6 shows the six measurement results for height for each part. The measured average values of the parts are shown in Fig. 7. Based on observation of the front, top and side views and measurement of the dimensions of each sample, the following conclusions were derived. (a) Sample 3 and sample 6 have obvious defects on the top, the deviation between their measured values is very large. (b) When the slice thickness H_s is slightly smaller than the nozzle diameter D, the formed height H of the deposition sample is basically equal to the design size (as samples 1 and 2); When the slice thickness H_s is greater than the nozzle diameter D, the height H of the formed sample is significantly smaller than the design size (as sample 4 and 5), because of the reduction in the number of printing layers. (c) When the printing speed V_p was increased from 2 mm/s to 2.5 mm/s, the formed wall thickness W_t of samples decreased significantly. The wall thickness of sample 1 is 10.9 mm and that of sample 4 is 8.35 mm, both of which are obviously larger than the design size of 6.5 mm. However, the wall thickness of samples 2 and 5 is basically equal to the design size of 6.5 mm. The main reason is that the printing speed of 2 mm/s does not match the ceramic extrusion speed. Because of the low printing speed, the extruded ceramic is excessively piled and spreads at the bottom of the nozzle, which leads to the width of each clay filament after deposition being much larger than the set filling gap. Finally, the wall thickness of the formed sample is larger than the design size. When the printing speed V_p is 2.5 mm/s, there is no excessive piling and spreading of the extruded clay. The width of each clay filament after deposition just meets the set filling gap, so the wall thickness of the formed sample is basically equal to the design size. (d) When the printing speed V_p was increased from 2 mm/s to 2.5 mm/s, there was only little change in the formed side length (L_s) of the sample. The side lengths of samples 2 and 5 measure 61.5 mm and 61.3 mm respectively, that is basically equal to the design size of 60 mm, and the relative error is 2.1 %. However, the side lengths of samples 1 and 4 measure 65.3 mm and 66.3 mm respectively, which are obviously larger than the designed size, and the relative error is 10 %. The main reason is that the printing speed of 2 mm/s is lower than the ceramic extrusion speed of 2.5 mm/s, which results in the clay filaments pushing against each other and spreading to both sides. Finally, the side length of the formed parts is larger. (e) When the printing speed is 3 mm/s, there are obvious morphological defects on the top of samples 3 and 6. Because the printing speed V_p is higher than the extrusion speed V_e of the clay filament, the extruded clay filament cannot fully contact the surface of the deposited layer during the deposition process. Under the action of extrusion pressure, the phenomenon of disordered deposition of the clay filament occurred and the deposition size error increased. With the increase in the number of deposited layers, the accumulated error is significant, and finally an irregular morphological defect is generated on the top of the formed sample.

Fig. 8 shows a partial enlarged view of the sample. It can be seen that the surface of the forming part has a remarkable layer-by-layer stacked line morphology. The bonding state between each layer is very good without obvious pores and cracks. But the forming quality is poor at the junction between the starting point and the ending point of the printing trajectory of each layer, and there is an obvious occlusal phenomenon. However, other corner shapes of the sample are regular. On the top layer of the sample being deposited, the forming surface is relatively flat, and the corner has obvious rectangular geometric characteristics.

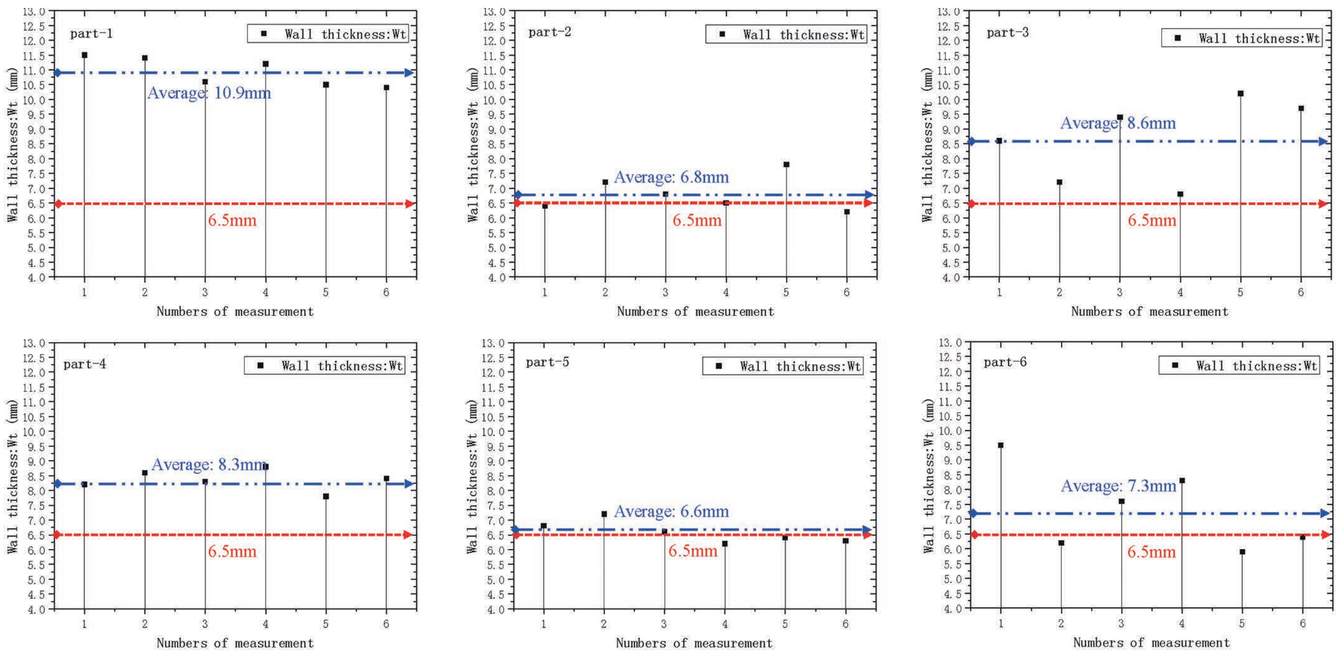

Fig. 4: The six measurement results for wall thickness in each part.

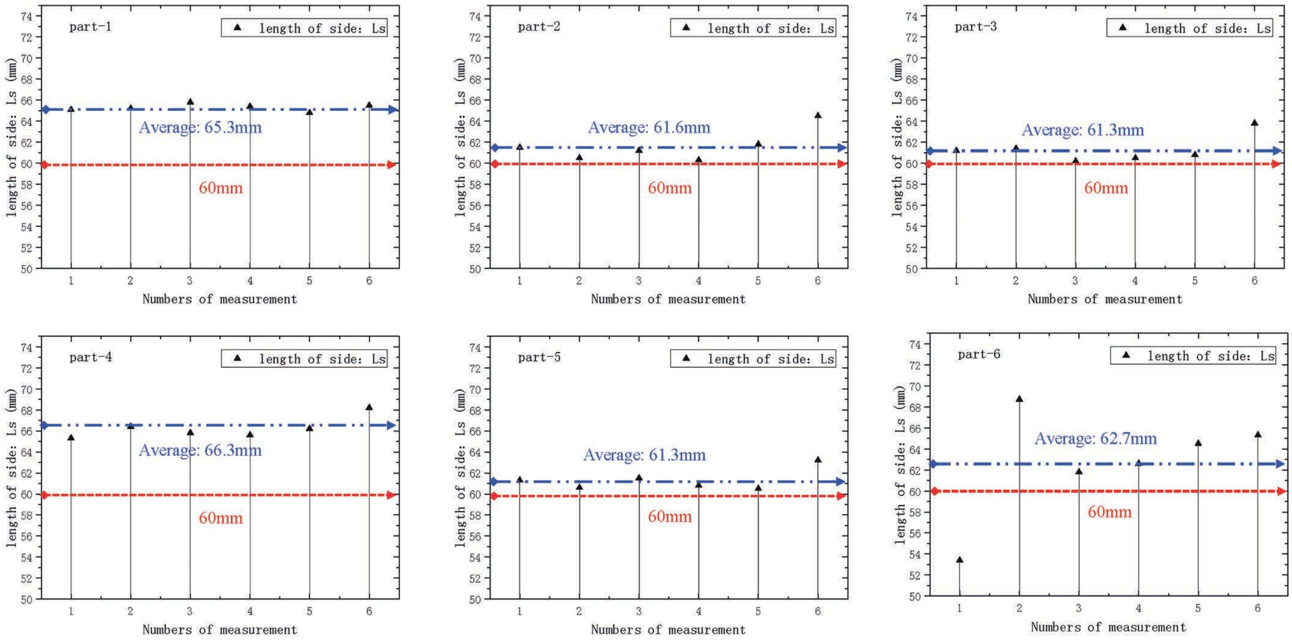

Fig. 5: The six measurement results for length of side in each part.

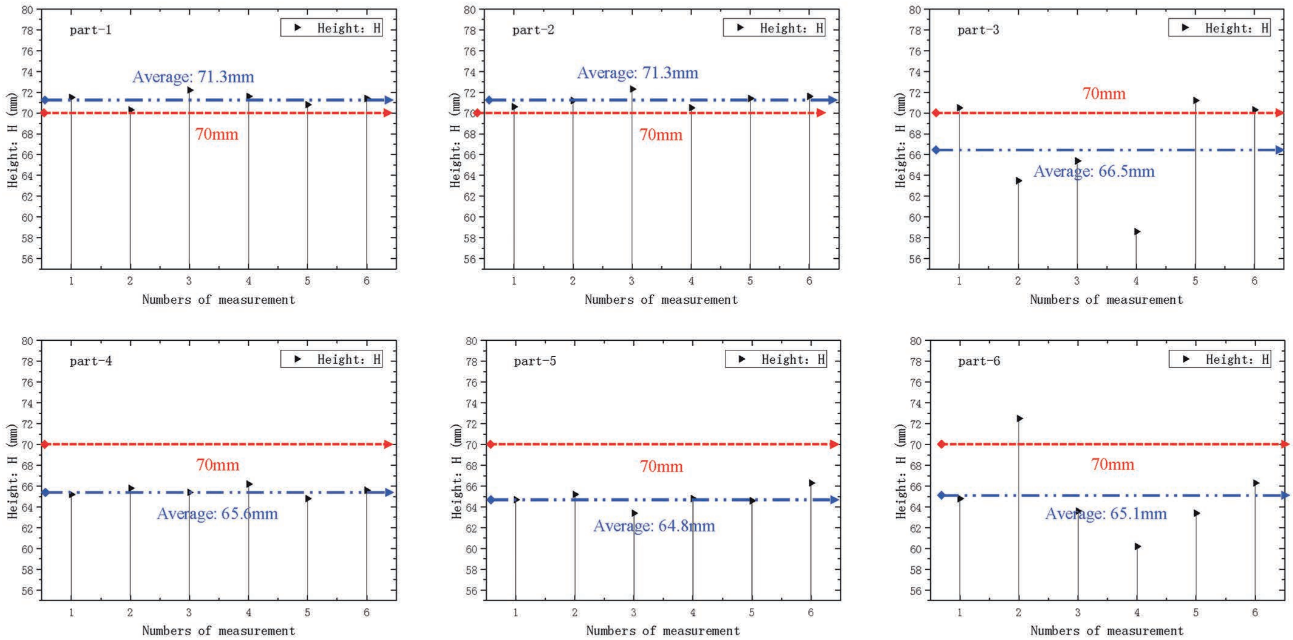

Fig. 6: The six measurement results for height in each part.

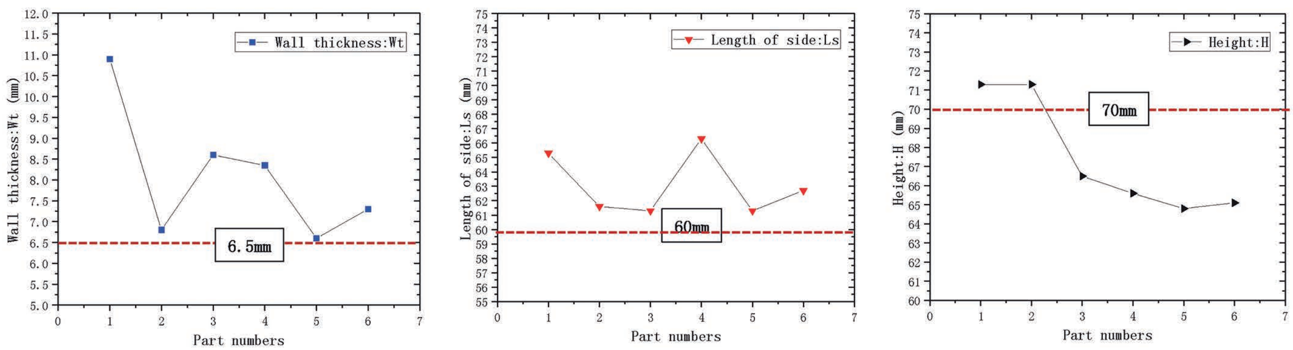

Fig. 7: The data point graph of measuring average value.

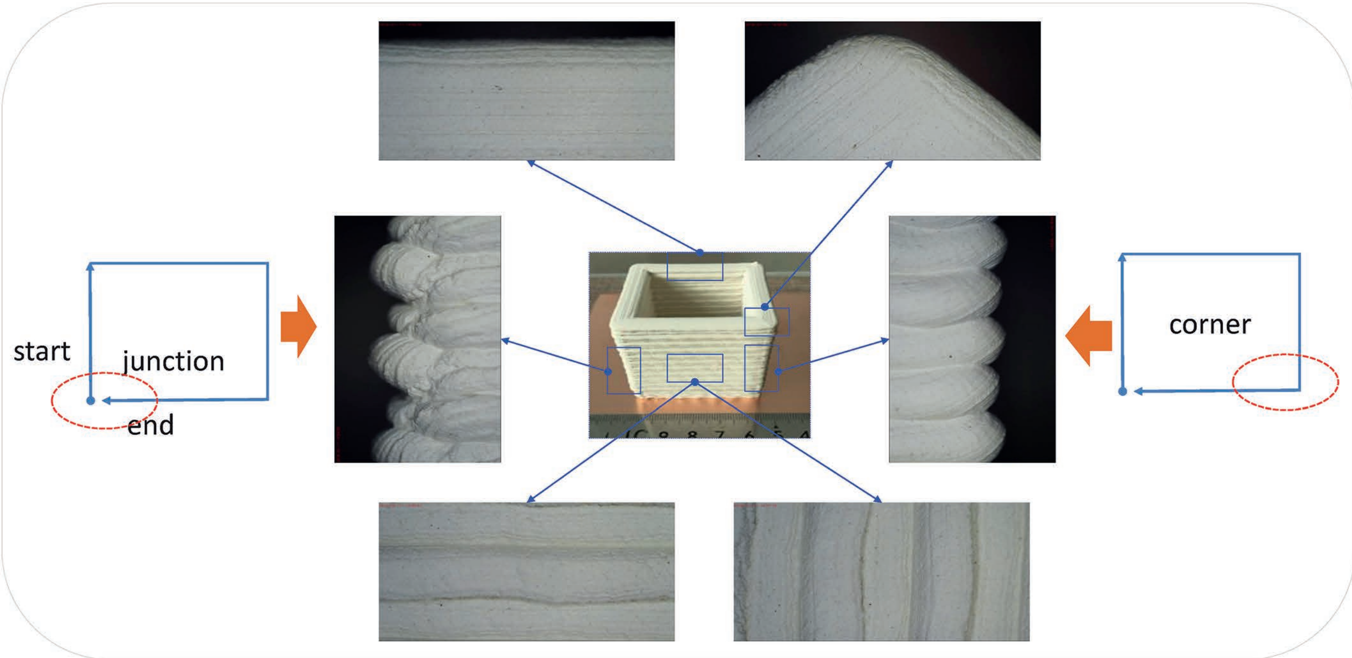

Fig. 8: Enlarged view of the formed sample.

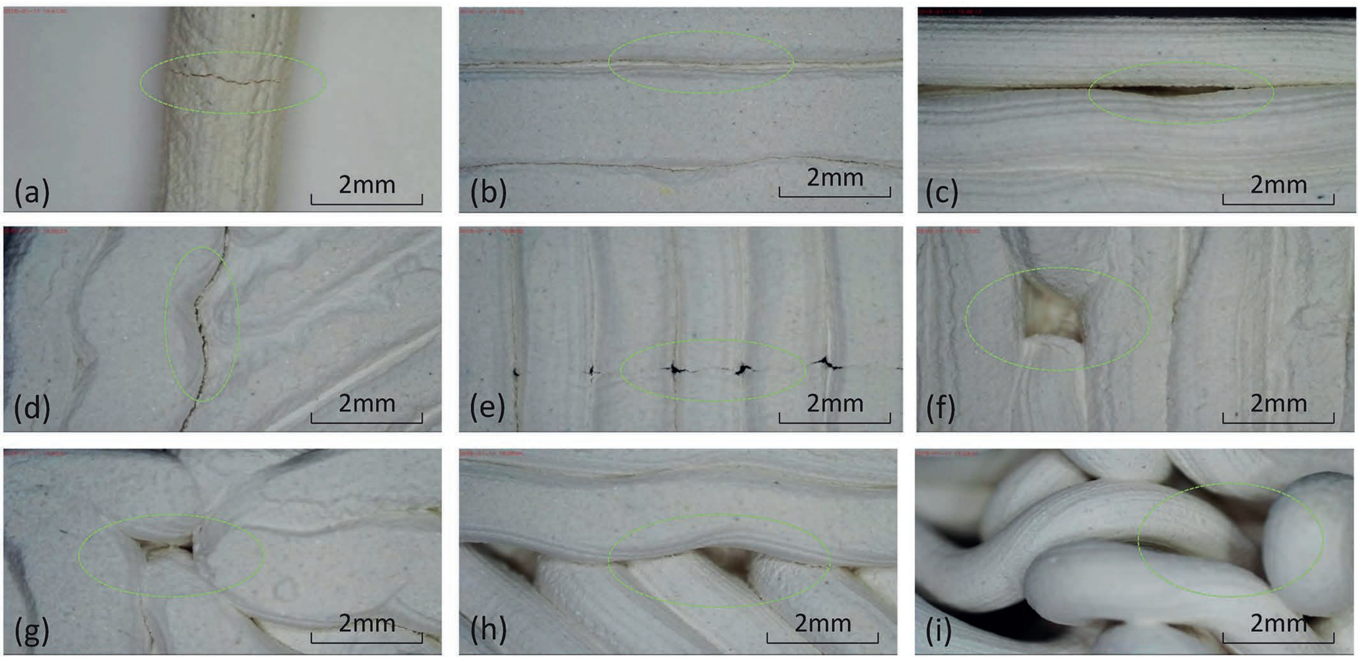

Fig. 9: The defect type in the printed parts a) the tiny crack defect in the single clay filament b) d) the small crack defect between adjacent deposited layers c) e) the porosity defects between adjacent deposited layers f) g) the hole defects existing at the junction of many clay filaments h) i) irregular morphological defects of the clay filament.

From the comparison and analysis of the appearance and the bonding quality of the parts formed with different process parameters in Fig. 7, it can be concluded that the formed parts have different types of defects. Fig. 9 shows the types of defects existing in the 3D-printed ceramic parts. A tiny crack defect of the single clay filament is shown in Fig. 9 a). A small crack defect between adjacent deposited layers is shown in Figs. 9 b) and d). Figs. 9 c) and e) show the porosity defects between layers deposited adjacent to each other. Figs. 9 f) and g) show hole defects existing at the junction of clay filaments. An irregular morphological defect of the clay filament after disordered deposition is shown in Figs. 9 h) and I). Analysis of the causes of these defects shows these are as follows: a) The ceramic materials contain a small amount of impurity particles, when the clay is extruded from the nozzle under non-uniform stress; a small crack is produced when the clay filament is deposited. b) Because the slice thickness H_s is greater than the diameter of the single clay filament, the deposited clay filaments of adjacent layers cannot be fully compacted, leading to tiny cracks being generated between the adjacent layers. c) The clay materials are not

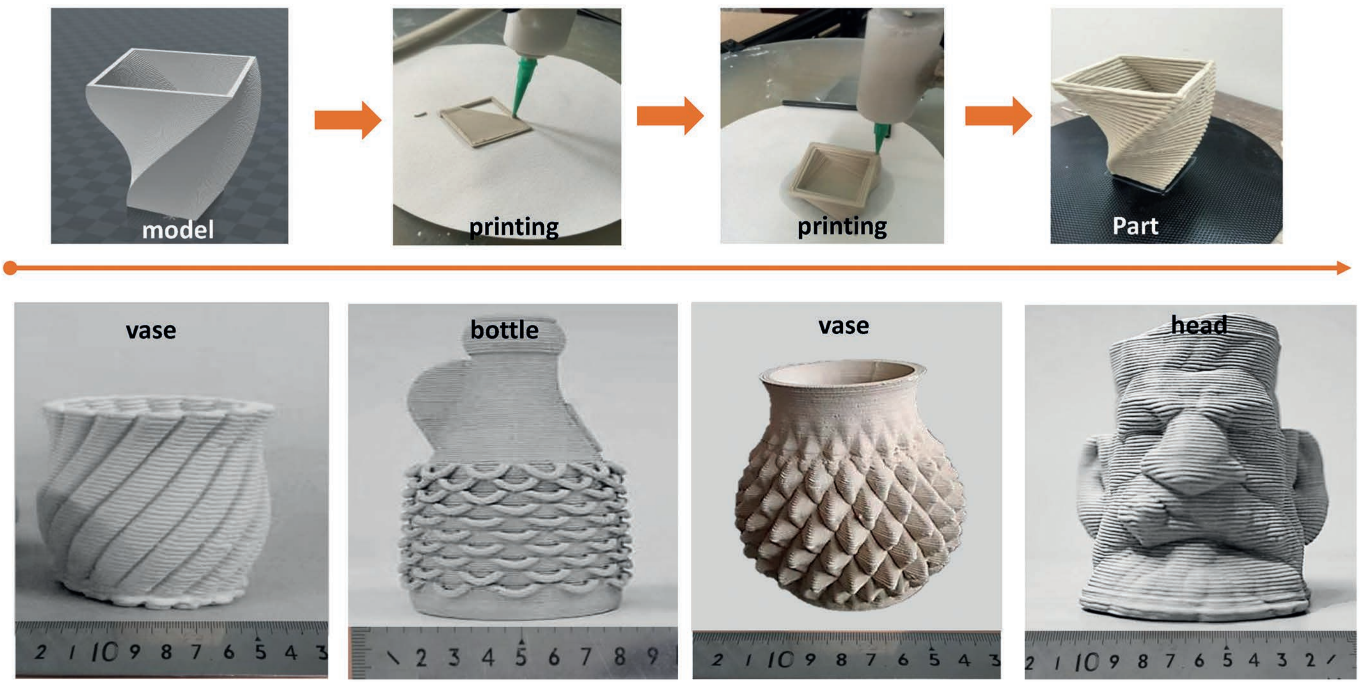

Fig. 10: The deposition of various ceramic original bodies.

mixed thoroughly, and a large amount of air is contained inside the clay. When the clay materials are extruded from the nozzle, the air is expelled from the local area of clay to form air bubbles. The pore defects are formed after the bubbles burst. d) Owing to its spreading property, the clay is relatively weak, when the clay filaments are connected in the junction area, the gap cannot be filled completely, and a hole defect is produced. e) Because the extrusion speed and the printing speed do not match, the extruded clay filament cannot fully contact the surface of the deposited layer during the deposition process. The disordered deposition of clay filament appears, leading to irregular morphological defects being generated.

On the basis of the above experiments and analysis, a series of 3D printing experiments was carried out. Fig. 10 shows the different printed ceramic models (vase, bottle and head). It can be seen that the shapes of various ceramic original bodies are complex and the contours are clearly defined, which basically meet the precision requirements of ceramic works. The feasibility of the clay 3D printing technique is verified.

V. Conclusions

(1) A novel ceramic clay 3D printing technology is proposed to fabricate ceramic parts by means of continuous extrusion and deposition of clay layer by layer. The structure, nozzle extrusion device and motion control module of 3D printing system have been developed.

(2) The appearance and the bonding quality of the parts formed with different process parameters are compared and analyzed. The types of defects (tiny cracks, porosity, holes and irregular morphology) and the causes of the defects are explored and summarized.

(3) The printing speed should match the extrusion speed of the ceramic clay. If the printing speed is lower than the extrusion speed, the clay filaments push against each other and spread to both sides. Conversely, if the printing speed is higher than the extrusion speed, the extruded clay filament cannot fully contact the surface of the deposited layer and the phenomenon of disorderly deposition occurs.

(4) The different original ceramic parts have been successfully fabricated; they have a complex shape and clear contours. The printing results basically meet the precision requirements for ceramic works. The feasibility of the clay 3D printing technique is verified.

Acknowledgement

This work was financially supported by the National Natural Science Foundation of China (51305128), funded by the key scientific and technological project of Henan province (192102210055), and the key scientific research projects of the colleges and universities of Henan province (18A4600050). I thank the reviewers for their helpful comments.

References

1 Eckel, Z.C., Zhou, C., Martin, J.H., Jacobsen, A.J., Carter, W.B., Schaedler, T.A.: Additive manufacturing of polymer-derived ceramics, *Science*, **351**, 58 – 62, (2016).

2 Costa, E.C., Duarte, J.P., Bártolo, P.: A review of additive manufacturing for ceramic production, *Rapid Prototyping J.*, **23**, 954 – 963, (2017).

3 MacDonald, E., Wicker, R.: Multi process 3D printing for increasing component functionality, *Science*, **30**, [353], 1512 – 1520, (2016).

4 Zhong, G., Vaezi, M., Pan, L.L., Yang, S.: Characterization approach on the extrusion process of bioceramics for the 3D printing of bone tissue engineering scaffolds, *Ceram. Int.*, **43**, 13860 – 13868, (2017).

5 Hwa, L.C., Rajoo, S., Noor, A.M., Uday, M.B.: Recent advances in 3D printing of porous ceramics: A review, *Curr. Opin. Solid. State. Mater. Sci.*, **21**, 323 – 347, (2017).

6 Gualtieri, T., Bandyopadhyay, A.: Additive manufacturing of compositionally gradient metal-ceramic structures: stain-

less steel to vanadium carbide, *Mater. Design.*, **139**, 419 – 428, (2018).

7 Chartier, T., Dupas, C., Lasgorceix, M.: Additive manufacturing to produce complex 3D ceramic parts, *J. Ceram. Sci. Technol.*, **6**, 95 – 104, (2014).

8 Criales, L.E., Arısoy, Y.M., Özel, T.: Sensitivity analysis of material and process parameters in finite element modeling of selective laser melting of Inconel 625, *Int. J. Adv. Manuf. Technol.*, 1 – 14, (2016).

9 He, R., Liu, W., Wu, Z., An, D., Huang, M., Wu, H., Jiang, Q., Ji, X., Wu, S., Xie, Z.: Fabrication of complex-shaped zirconia ceramic parts via a DLP- stereo-lithography-based 3D printing method, *Ceram. Int.*, **44**, [3], 3412 – 3416, (2018).

10 Chen, Z., Ouyang, J., Liang, W., Yan, Z.-c., Stadler, F., Lao, C.: Development and characterizations of novel aqueous-based LSCF suspensions for inkjet printing, *Ceram. Int.*, **44**, [11], 13381 – 13388, (2018).

11 Deckers, J., Vleugels, J., Kruth, J.P.: Additive manufacturing of ceramics: A review, *J. Ceram. Sci. Technol.*, **5**, [4] 245 – 260, (2014).

12 Yun, J.S., Park, T.W., Jeong, Y.H., Cho, J.H.: Development of ceramic-reinforced photopolymers for SLA 3D printing technology, *Appl. Phys. A.*, **122**, [629],1 – 6, (2016).

13 Deckers, J., Vleugels, J., Kruth, J.P.: Additive manufacturing of ceramics: A review, *J. Ceram. Sci. Technol.*, **5**, [4], 245 – 260, (2014).

14 Hwa, L.C., Rajoo, S., Noor, A.M., Ahmad, N., Uday, M.B.: Recent advances in 3D printing of porous ceramics: A review, *Curr. Opin. Solid. State. Mater. Sci.*, **21**, 323 – 347, (2017).

15 Lian, Q., Sui, W., Wu, X., Yang, F., Yang, S.: Additive manufacturing of ZrO_2 ceramic dental bridges by stereolithography, *Rapid Prototyping J.*, **24**, [1], 114 – 119, (2018).

16 Fu, Y., Xu, G., Chen, Z., Wang, D., Lao, C.: Multiple metals doped polymer-derived SiOC ceramics for 3D printing, *Ceram. Int.*, **44**, [10], 11030 – 11038, (2018).

17 Chen, Z.G., Li., Y., Li, J.J., Liu, C.B., Lao, C.S., Fu, Y.L., Liu, C.Y., Li, Y., Wang, P., He, Y.: 3D printing of ceramics: A review, *J. Eur. Ceram. Soc.*, **39**, 661 – 687, (2019).